Supplementary Information

Highly efficient interfacial hole transporting tunnel of bipyridine semiconductor for perovskite solar cells

Jinxue Zhang[a,b], Fantai Kong[a*], Yaole Peng[a,b], Chundie Zhao[a,b], Shuanhong Chen[a], Rahim Gradari[c], Wenjun Liu[a]

[a] Key Laboratory of Photovoltaic and Energy Conservation Materials, Institute of Solid State Physics, Hefei Institute of Physical Science (HFIPS), Chinese Academy of Sciences, Hefei, 230031, China.

[b] University of Science and Technology of China, Hefei, 230026, China

[c] Computational Chemistry Laboratory, Department of Organic and Biochemistry, Faculty of Chemistry, University of Tabriz, 5166616471, Tabriz, Iran

*Email: kongfantai@163.com

Contents

1. Materials and reagents

4,4'-([2,2'-bipyridine]-4,4'-diyl)bis(N,N-bis(4-methoxyphenyl)aniline)(4-BA) was synthesized via a Suzuki coupling reactoion. All other reagents were obtained from commercial companies. Methylammonium Iodide (MAI), PbI_2, formamidinium iodide (FAI), CsI, and methylammonium Chloride (MACl) were purchased from Xi'an Polymer Light Technology Co., Ltd. Dimethyl formamide (DMF), Dimethyl sulfoxide (DMSO) and isopropyl alcohol (IPA) were purchased from China National Medicines Corporation Ltd. 4,4'-((4-bromophenyl)methylene)bis(methoxybenzene) and 4-methoxy-N-(4-methoxyphenyl)-N-(4-(4,4,5,5-tetramethyl-1,3,2-dioxaborolan-2-yl)phenyl)aniline were bought from Inno-Chem Science & Technology Co., Ltd..

2. Synthetic routes

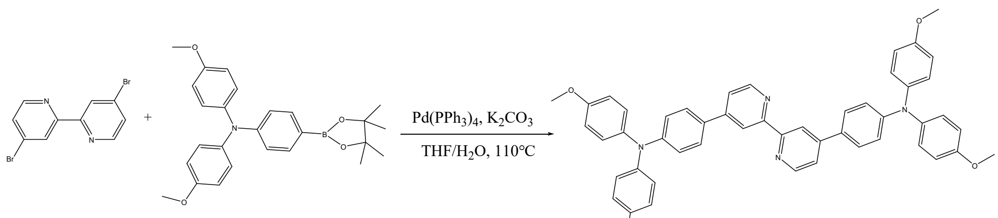

1 2 4-BA

Scheme S1. Synthetic route of 4-BA.

Synthesis of 4-BA. 4,4'-dibromo-2,2'-bipyridine (0.139g, 0.443 mmol), 4-methoxy-N-(4-methoxyphenyl)-N-(4-(4,4,5,5-tetramethyl-1,3,2-dioxaborolan-2-yl)phenyl)aniline (0.439 mg, 1.02mmol), $Pd(PPh_3)_4$ (16 mg, 0.014 mmol) , and K_2CO_3 solution(2mol/L, 10mL) in anhydrous toluene (10 mL) were placed in a Schlenk tube under nitrogen atmosphere and was stirred at 110°C for 48 h. After cooling, the reaction was quenched with water, and then extracted with dichloromethane. The organic layer was washed with brine and dried over anhydrous Na_2SO_4. After evaporation of the solvent, the residue was purified by column chromatography over silica gel, with dichloromethane: Petroleum etheras (2:1) as the solvent. 4-BA was obtained as a yellow solid (427 mg, yield 74%). ^1H NMR (600 MHz, chloroform-*d,* δ, ppm): 8.50 (d, *J* = 7.7 Hz, 2H), 8.01 (d, *J* = 8.4 Hz, 4H), 7.85 (t, *J* = 7.8 Hz, 2H), 7.69 (d, *J* = 7.9 Hz, 2H), 7.14 (d, *J* = 8.5 Hz, 7H), 7.06 (d, *J* = 8.4 Hz, 4H), 6.88 (d, *J* = 8.5 Hz, 7H), 3.84 (s, 12H). ^{13}C NMR (151 MHz, chloroform-*d*, δ, ppm): 156.06 (d, *J* = 4.4 Hz), 140.71, 137.39, 127.60, 126.82, 120.20, 119.30, 118.53, 114.74, 55.53. HRMS-ESI (m/z): $[M + H]^+$ Calcd. For ($C_{50}H_{42}N_4O_4$), 763, found: 763.

3. Perovskite solar cells fabrication

The etched FTO glass substrates were cleaned with acetone, isopropyl alcohol, and deionized water for 20 min, respectively and finally treated for 20 min by ultraviolet ozone. The titanium diisopropoxide bis(acetylacetone)/isopropanol solution was sprayed on FTO glass and then heated at 450 °C for 1 h to prepare the c-TiO_2 layer. 30 μL of the TiO_2 slurry was then spin-coated on the c-TiO_2 layer and annealed at 500 °C for 30 min to prepare m-TiO_2. The perovskite film was fabricated by a one-step spin coating method. The 1.4 mol/L $Cs_{0.05}FA_{0.95}MA_{0.05}PbI_3$ solution was prepared with PbI_2 0.6777g, FAI 0.2287g, MAI 0.0111g, CsI 0.0182g, MACl 0.0188g and DMSO: DMF= 300 μL: 700μL. The solution of perovskite was spin-coated at 1000 rpm for 10 s and 5000 rpm for 30 s on the electron layer then extracted with chlorobenzene as antisolvent and annealed at 150 °C for 10 min to get the perovskite film. Then the Spiro-OMeTAD layer solution containing 73.5 mg of Spiro-OMeTAD, 1 mL chlorobenzene, 29 μL *t*BP, 17 μL bis(trifluoromethane)sulfonimide lithium salt (196 mg/379 μL acetonitrile) and 8 μL FK 209 Co

(III) TFST salt (99 mg/263 μL acetonitrile) was spin-coated at 3000 r min^{-1} for 20 s in dry air atmosphere and the gold electrode was deposited by thermal evaporation.

4. Characterization and measurements

The NMR spectra were obtained from a Bruker AV-600 NMR (Germany) spectrometer (in $CDCl_3$). The software used is Guassian 09, based on the B3LYP6-31G basis set, to calculate the optimized structure of the molecule, the intramolecular dihedral angle, the highest occupied molecular orbital (HOMO) and the lowest unoccupied molecular orbital (LUMO) distribution and electrostatic potential distribution (ESP). The curves of XRD were measured by X-ray diffraction (Rigaku Smartlab 9kW). Confocal photoluminescence (PL) maps were obtained with a confocal Raman microscope (Thermo-Fisher). UV-vis absorption spectra were recorded with a UV spectrophotometer (Hitachi U-3900H). Surface and cross-sectional images were acquired by field emission scanning electron microscopy (SU8220, Hitachi). Steady-state PL spectra were obtained using (QM400-TM). The energy levels and chemical composition of the films were analyzed using ultraviolet photoelectron spectroscopy (UPS) and X-ray photoelectron spectroscopy (Thermo Scientific, ESCALAB 250Xi). CV tests were performed with a CHI66d electrochemical analyzer (Shanghai CH Instruments, China). TGA was performed with TGA-Q5000IR and DSC measurements were performed with a DSC Q2000 instrument. The instrument model of the scanning electron microscope used was GeminiSEM 450. Water contact angles were menaured by OCA15E (Datephysics). Photocurrent-voltage (*J*-*V*) characteristics are measured under AM 1.5 illumination by a 3A grade solar simulator (Newport, USA, 94043A). IPCE was performed on IPCE measurement kit (Newport, USA).

The CV tests were measured by CHI66d electrochemical analyzer (Shanghai CH Instruments, China) in a three-electrode cell. The working electrode was a glassy carbon electrode, used in conjunction with a Pt wire counter electrode and a saturated calomel reference electrode. An amount of 0.1 mol/L tetrabutylammonium hexafluorophosphate ($TBAPF_6$) solution in CH_2Cl_2 was used as the supporting electrolyte. The Fc/Fc^+ redox couple was used as an external potential reference. The scanning rate was 50 mV/s.

TGA was performed with TGA-Q5000IR at a heating rate of 10 °C/min from 50 °C to 700°C under a nitrogen atmosphere. DSC measurements were performed with a DSC Q2000 instrument at a heating rate of 5 °C/min under a nitrogen atmosphere from 50°C to 200°C.

The space-charge-limited current (SCLC) method was used to evaluate hole mobility. The device structure of FTO/PEDOT:PSS(Poly(3,4-ethylenedioxythiophene)/poly (styrenesulfonate))/HTM with/without 4-BA/Au. The limited current of space-charge can be labeled by calculation below:

$$J^{1/2} = 9\mu\varepsilon_0\varepsilon_r V^2 / 8d^3$$

where J is the current density, μ is the hole mobility, ε_0 is the vacuum permittivity (8.85×10^{-12} F/m), ε_r is the dielectric constant of the material, V is the applied bias, and L is the film thickness. For defect density measurement, the n_{trap} values were calculated by calculation below:

$$n_{trap} = 2\varepsilon\varepsilon_0 V_{TFL} / eL^2$$

Where ε is the relative dielectric constant of perovskite (32 F/m), L is the thickness of the perovskite film, e is the elementary charge of the electron ($e = 1.6\times10^{-19}$ C), and ε_0 is the vacuum permittivity.

5.Figures and tables.

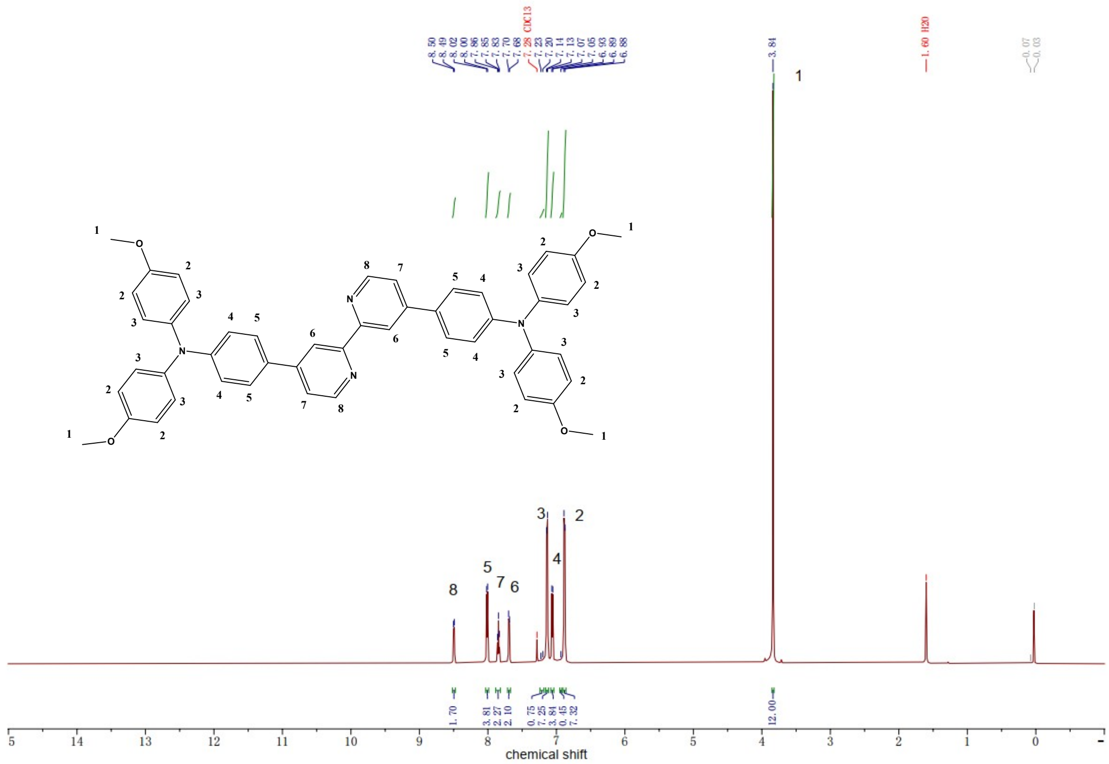

Fig S1. ^{1}H-NMR spectrum of 4-BA in $CDCl_3$.

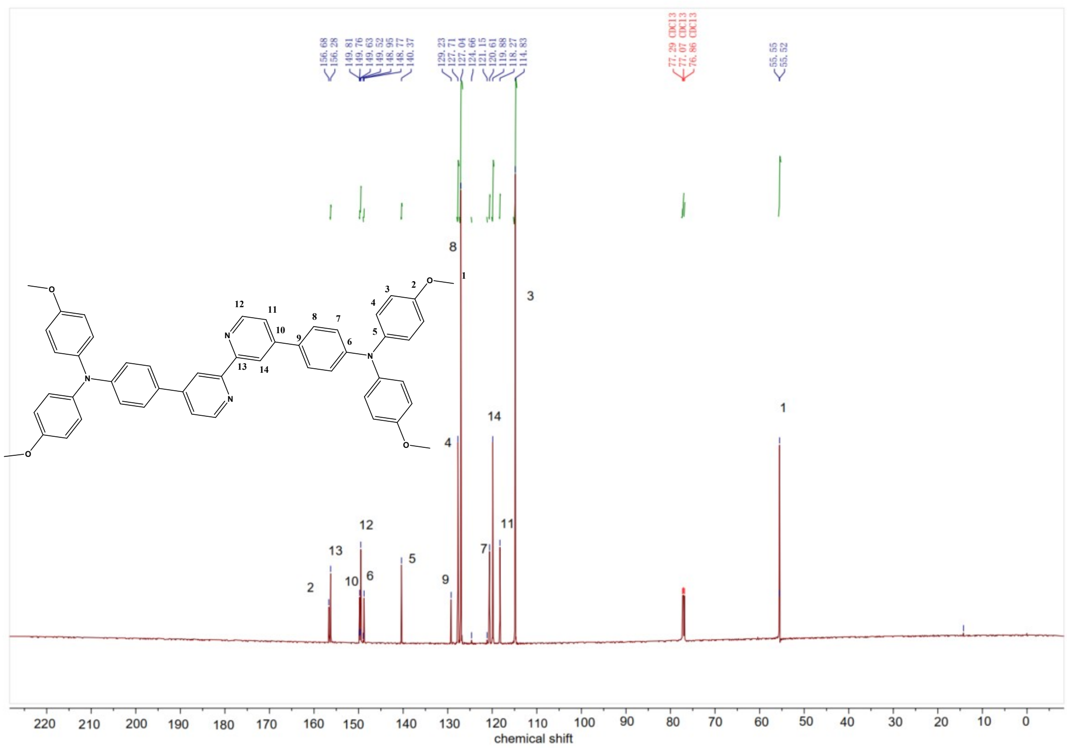

Fig. S2. ^{13}C-NMR spectrum of 4-BA in $CDCl_3$.

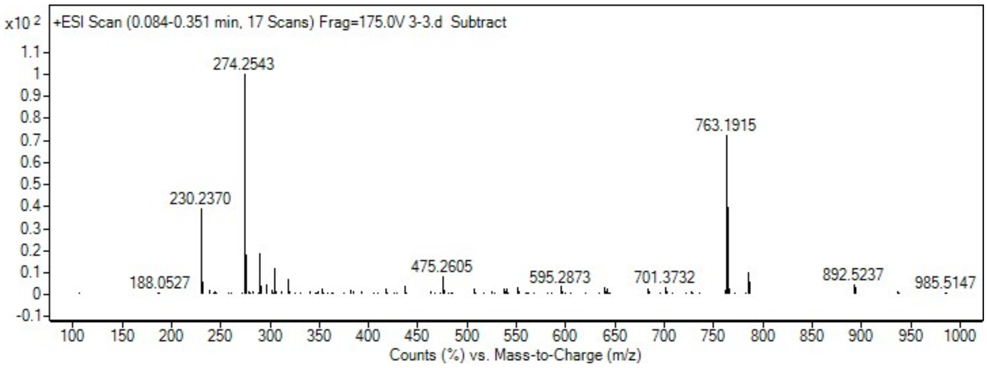

Fig. S3. High resolution mass spectrometry of 4-BA.

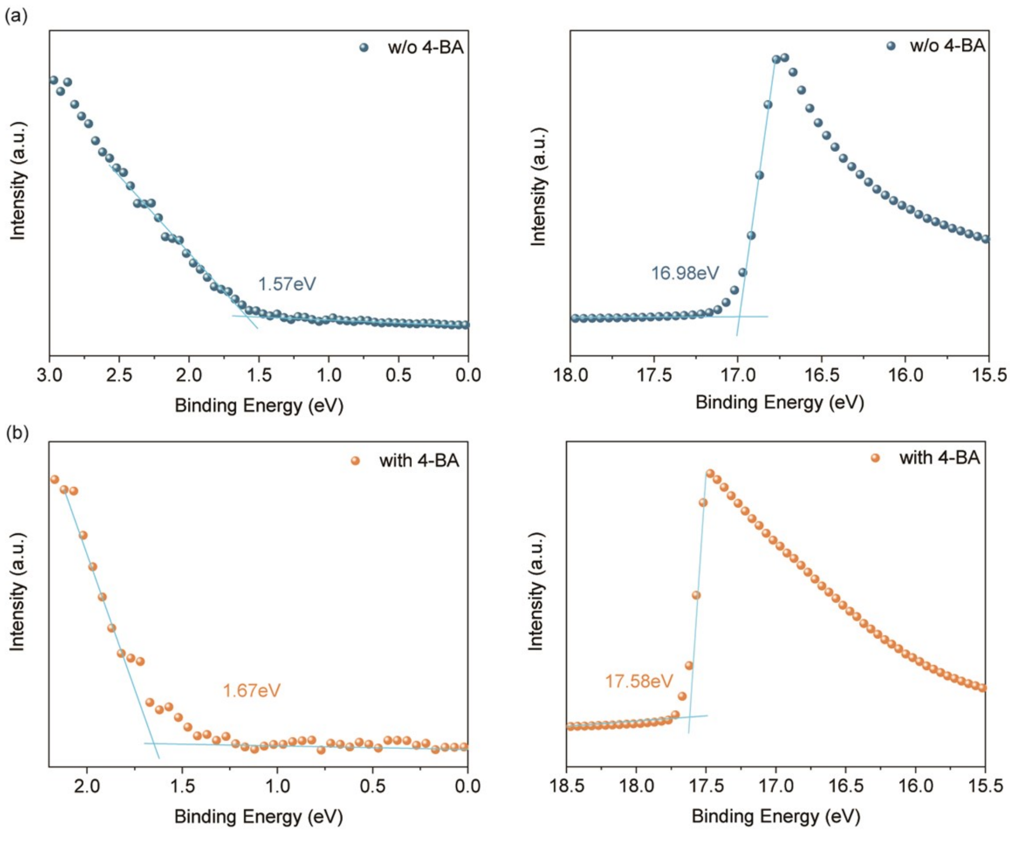

Fig. S4. UPS spectra of perovskite films with/without 4-BA.

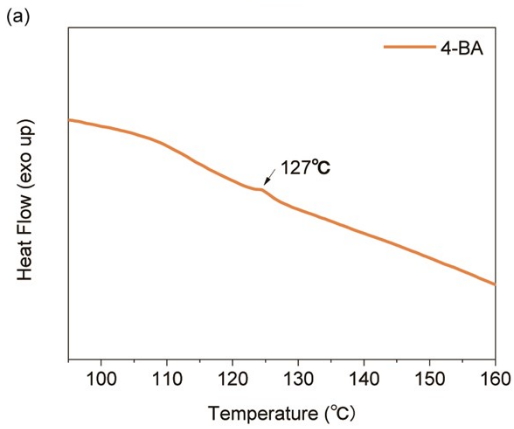

Fig. S5. (a) The DSC of 4-BA under nitrogen at a heating rate of 5 ℃/min.

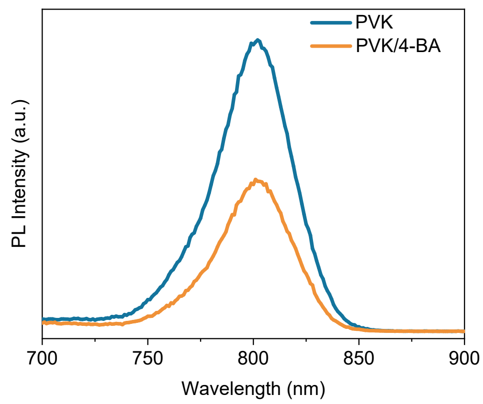

Fig. S6 Steady-state PL spectra of perovskite films with/without 4-BA.

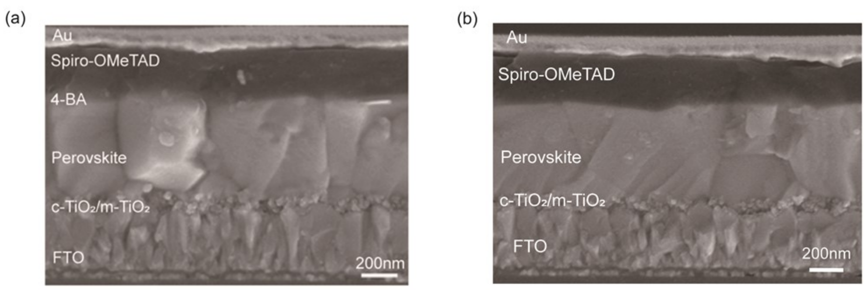

Fig. S7 (a) Cross-sectional SEM image of the device with 4-BA. (b) Cross-sectional SEM image of the device without 4-BA.

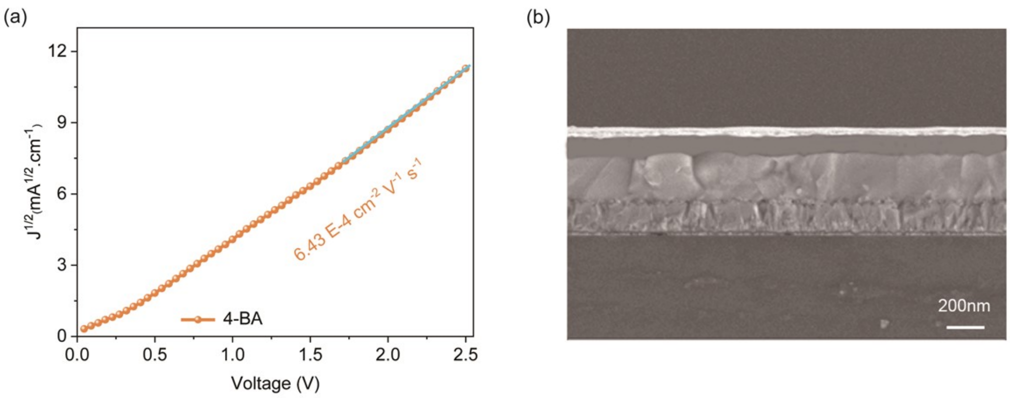

Fig. S8 (a)The space-charge limited current (SCLC) curve of 4-BA only device. (b) Cross-sectional SEM image of the FTO/Perovskite/4-BA/Au.

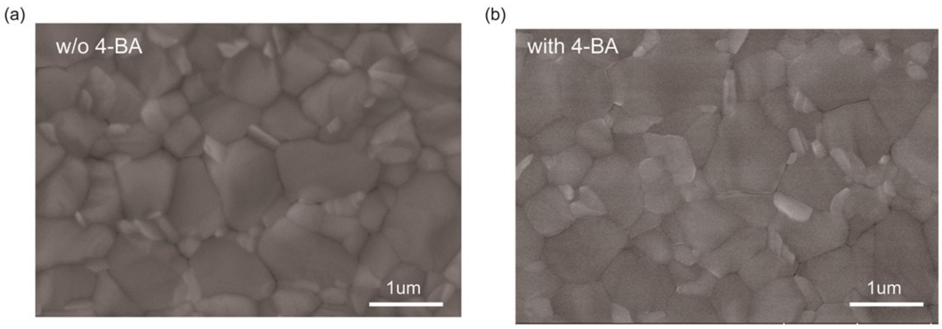

Fig. S9. Top-view SEM images of perovskite films with/without 4-BA

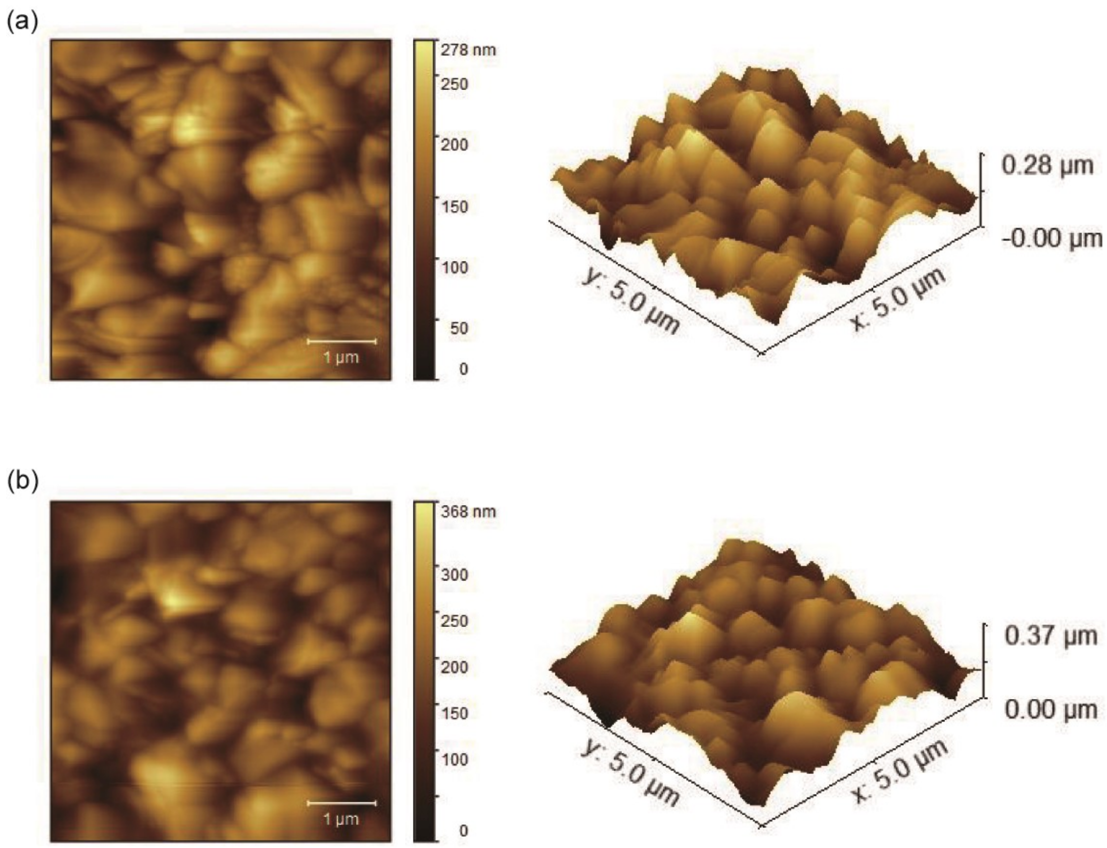

Fig. S10 (a)The AFM images of perovskite film with 4-BA. (b) The AFM images of perovskite film without 4-BA.

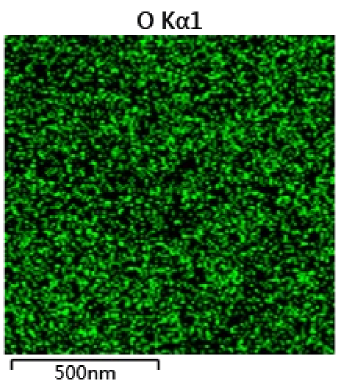

Fig. S11 O element mapping of the perovskite film with 4-BA.

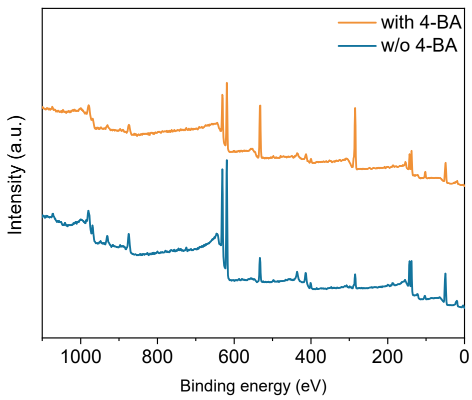

Fig. S12 XPS spectra of perovskite with/without 4-BA.

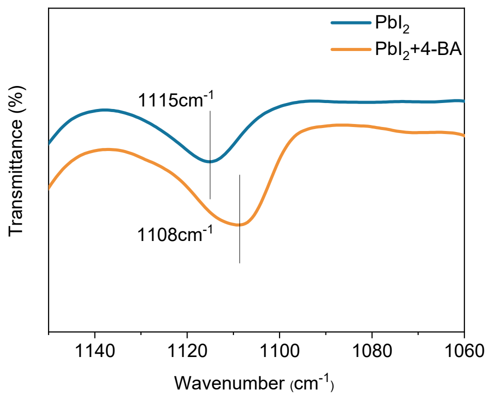

Fig. S13 FT-IR spectra of PbI_2 and PbI_2 mixtures with 4-BA.

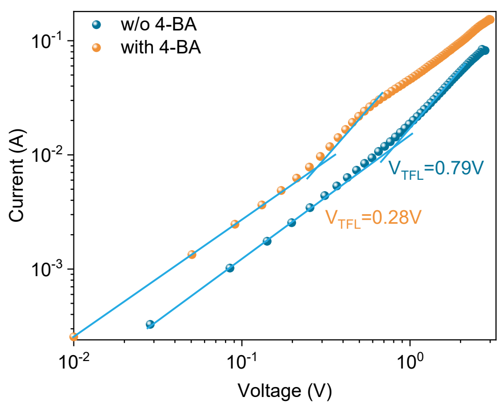

Fig. S14 Trap density of perovskite films measured with/without 4-BA by use electron only device *J*-*V* curves.

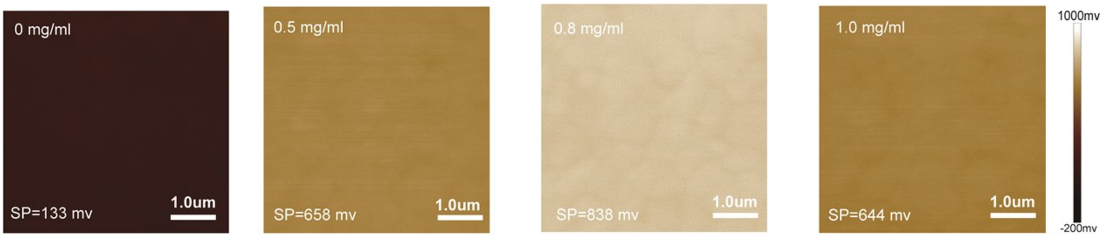

Fig. S15 The surface potential of devices with 4-BA at different concentrations.

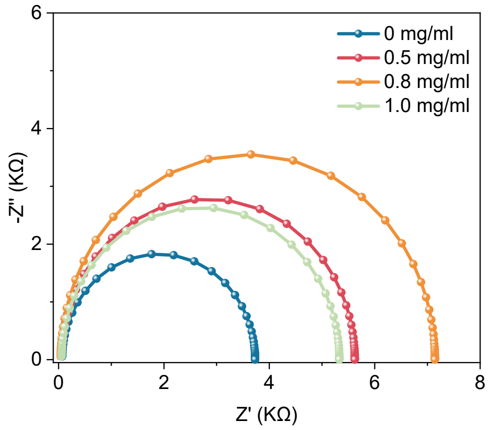

Fig. S16 The EIS of devices with 4-BA at different concentrations.

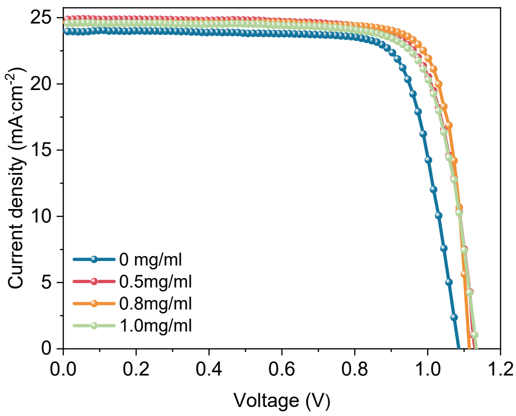

Fig. S17 The *J*–*V* curves of devices with 4-BA at different concentrations.

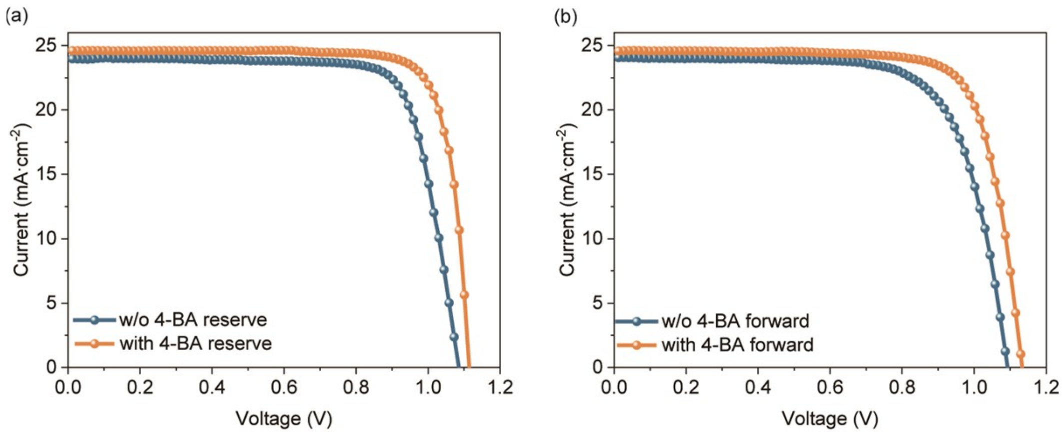

Fig. S18 (a) Reserve scan *J–V* curves of devices with/without 4-BA. (b) Forward scan *J–V* curves of devices with/without 4-BA.

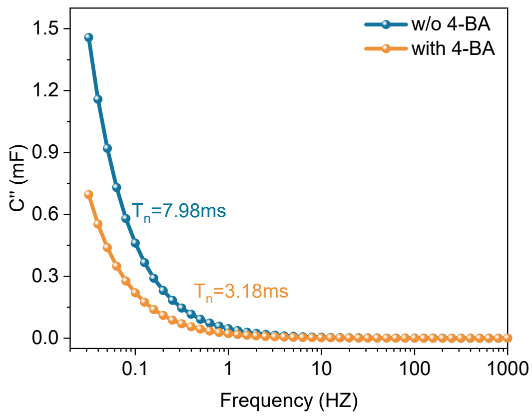

Fig. S19. Relationship between imaginary capacitance and frequency of PSCs device with/without 4-BA.

Table S1 Calculated parameters of devices w/o 4-BA and with 4-BA (0.8mg/ml) from EIS.

Sample	R_s (Ω)	R_{ct} (Ω)
w/o 4-BA	40.4	39.3
with 4-BA	3453	7231

Table S2 The photovoltaic parameters with different concentrations of 4-BA.

concentration	V_{oc} (V)	J_{sc}(mA·cm^{-2})	FF(%)	PCE(%)
0	1.08	24.0	77.5	20.2
0.5	1.13	24.8	77.2	21.7
0.8	1.12	24.6	81.7	22.4
1.0	1.13	24.6	77.0	21.4